



# Advanced Synthesis & Catalysis

## Accepted Article

**Title:** Expanding the Scope of Enantioselective Halohydrin Dehalogenases – Group B

**Authors:** Emina Mehić, Lucija Hok, Qian Wang, Irena Dokli, Marina Svetec Miklenić, Zvezdana Findrik Blažević, Lixia Tang, Robert Vianello, and Maja Majerić Elenkov

This manuscript has been accepted after peer review and appears as an Accepted Article online prior to editing, proofing, and formal publication of the final Version of Record (VoR). This work is currently citable by using the Digital Object Identifier (DOI) given below. The VoR will be published online in Early View as soon as possible and may be different to this Accepted Article as a result of editing. Readers should obtain the VoR from the journal website shown below when it is published to ensure accuracy of information. The authors are responsible for the content of this Accepted Article.

**To be cited as:** *Adv. Synth. Catal.* 10.1002/adsc.202200342

**Link to VoR:** <https://doi.org/10.1002/adsc.202200342>

# Expanding the Scope of Enantioselective Halohydrin Dehalogenases – Group B

Emina Mehić,<sup>a</sup> Lucija Hok,<sup>a</sup> Qian Wang,<sup>b</sup> Irena Dokli,<sup>a</sup> Marina Svetec Miklenić,<sup>c</sup> Zvezdana Findrik Blažević,<sup>d</sup> Lixia Tang,<sup>b</sup> Robert Vianello,<sup>a,\*</sup> and Maja Majerić Elenkov<sup>a,\*</sup>

<sup>a</sup> Division of Organic Chemistry and Biochemistry, Ruđer Bošković Institute, Bijenička c. 54, 10000 Zagreb, Croatia  
E-mail: Robert.Vianello@irb.hr; Maja.Majerice.Elenkov@irb.hr

<sup>b</sup> University of Electronic Science and Technology, No.4, Section 2, North Jianshe Road, Chengdu, China

<sup>c</sup> Faculty of Food Technology and Biotechnology, University of Zagreb, Pierottijeva 6, 10000 Zagreb, Croatia

<sup>d</sup> Faculty of Chemical Engineering and Technology, University of Zagreb, Savska c. 16, 10000 Zagreb, Croatia

Received: ((will be filled in by the editorial staff))



Supporting information for this article is available on the WWW under <http://dx.doi.org/10.1002/adsc.201#####>.

**Abstract.** Halohydrin dehalogenases (HHDHs) possess an unnatural activity of introducing functionalities such as N<sub>3</sub>, CN, NO<sub>2</sub> etc., into a molecule through the ring-opening reaction of epoxides. The enantioselectivity of HHDHs is substrate-dependent and not always high enough for synthetic applications. B-group of HHDHs has been neglected in the past, due to observed low enantioselectivity based on performance on a relatively limited number of substrates. Extensive screening of substrates on HheB2 from *Mycobacterium* sp. GP1 and HheB from *Corynebacterium* sp. N-1074 was performed. Several highly enantioselective reactions were discovered ( $E > 200$ ), with HheB showing higher enantioselectivity and activity toward larger panel of substrates compared to HheB2. Enzymes HheB and HheB2

are highly homologous; they differ by only 4 residues. By using site-directed mutagenesis, residues 120 and 125 were found to be responsible for higher enantioselectivity of HheB compared to HheB2. Computational analysis supported experiments and provided evidence that kinetic and thermodynamic parameters of reactions within HheB enzymes are crucial in determining the observed enantioselectivities. Due to remarkable activity and enantioselectivity, B-group HHDHs emerged as a catalyst of choice for the synthesis of bulky tertiary alcohols, as shown in this work.

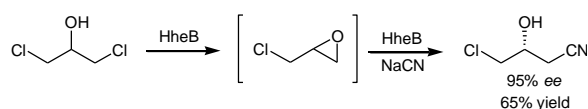
**Keywords:** biocatalysis; halohydrin dehalogenase; epoxides; kinetic resolution; molecular modelling

## Introduction

Epoxides are frequently used intermediates in the synthesis of optically active molecules. Enzymatic ring-opening by halohydrin dehalogenases (HHDHs, EC 4.5.1.-) has been intensively studied over the past years.<sup>[1]</sup> By using a variety of anionic nucleophiles, HHDHs can convert epoxides to  $\beta$ -substituted alcohols and oxazolidinones in a stereoselective fashion.<sup>[2]</sup> The main limitation in their application is a small number of existing enantioselective enzymes. A huge effort has recently been made in the discovery of wild-type HHDHs.<sup>[3]</sup> Unfortunately, this new collection did not yet provide an enzyme with a desirable enantioselectivity. For synthetic application, HheC from *Agrobacterium radiobacter* AD1 still remains the only wild-type HHDH with a high enantioselectivity,<sup>[1a,2b,4]</sup> whereas most of the other enzymes found in nature are either unselective or display only a moderate enantioselectivity toward tested substrates.<sup>[3,5]</sup> Although, the activity of HHDHs in general, is restricted to terminal epoxides, it has been found that the enzyme HheG exhibits activity towards 2,3-disubstituted epoxides.<sup>[5a,5f,5g]</sup> Based on

phylogenetic analysis, all known HHDHs are classified to seven groups, from A to G.<sup>[1b]</sup> Among the first discovered HHDHs are enzymes from *Corynebacterium* sp. N-1074 (HheB)<sup>[6]</sup> and *Mycobacterium* sp. GP1 (HheB2),<sup>[7]</sup> belonging to group B. Although isolated and characterized in 1999,<sup>[7a]</sup> the biocatalytic potential of HheB2 has not been broadly studied, mostly due to its apparently low enantioselectivity. A low  $E$  value was found for the conversion of *para*-nitro-2-bromo-1-phenylethanol to epoxide ( $E < 3$ ), with the slight preference towards (*S*)-enantiomer.<sup>[8]</sup> Cyanolysis of a series of structurally different aliphatic epoxides was catalysed with low to moderate enantioselectivity ( $E = 1-10$ ), yet high regioselectivity.<sup>[9]</sup> Based on the aforementioned research, HheB2 was considered as a regioselective enzyme, displaying a broad substrate range but low enantioselectivity.<sup>[10]</sup> In contrast, HheB from *Corynebacterium* sp. was found to catalyse highly enantioselective transformation of 1,3-dichloro-2-propanol to (*R*)-4-chloro-3-hydroxybutyronitrile (Scheme 1).<sup>[6b]</sup> This pioneering work has opened the door for the application of HHDHs ring-opening activity in biocatalysis in general. Even though this

research uncovered the stereoselective properties of HheB, it was not further explored on other substrates.



**Scheme 1.** Previous work done by Nakamura; HheB-catalysed conversion of 1,3-dichloro-2-propanol to (*R*)-4-chloro-3-hydroxybutyronitrile.<sup>[6b]</sup>

In recent years, by using structure-based site-directed and random mutagenesis methods, HheB-mutants with improved enantioselectivity in the conversion of 1,3-dichloro-2-propanol were constructed.<sup>[11]</sup> Besides, its crystal structure was solved,<sup>[12]</sup> revealing the familiar homotetrameric fold that share HHDHs from all subgroups.<sup>[13]</sup> HheB is highly homologous to HheB2, they differ by only 4 residues (Ile36/Phe36, Ala120/Thr120, Tyr124/Cys124 and Gln125/His125), of which 3 are in the active site and most likely responsible for the observed higher enantioselectivity (Figure 1). The goals of the present work were to evaluate substrate profile and the enantioselectivity of enzymes HheB2 and HheB, and to reveal experimentally which residue is responsible for apparently enhanced selectivity.

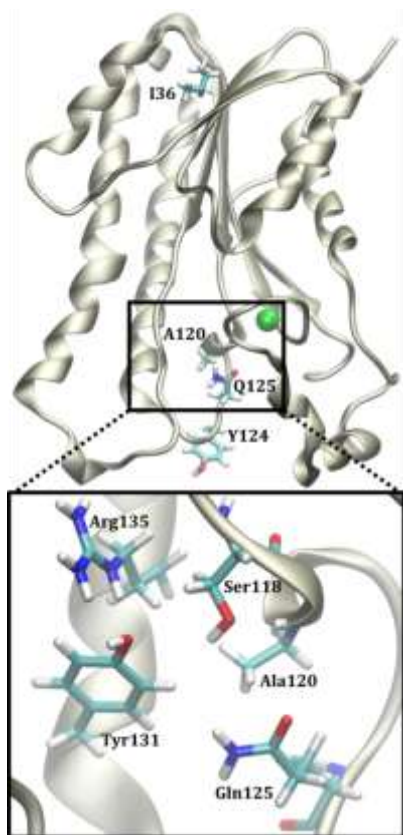


**Figure 1.** Location of HheB residues different from HheB2 with a halide site marked in green. Inset figure shows the active site residues Ser118, Tyr131 and Arg135. Ala120 and Gln125 are positioned close to the catalytic site.

## Results and Discussion

### Substrate scope

In spite of a very low enantioselectivity observed for HheB2 in the ring-opening reaction of several commercially available epoxides (Table 1), we continued our research by selecting a larger set of structurally different substrates, covering different number and nature of substituents on the oxirane ring. To probe the importance of the amino acid sequence differences in the active sites of HheB2 and HheB, we constructed four single mutants of HheB2 (Phe36Ile, Thr120Ala, Cys124Tyr and His125Gln), as well as a HheB that has incorporated all four mutations (Phe36Ile/Thr120Ala/Cys124Tyr/His125Gln).

**Table 1.** Enantioselectivity of HheB2 in the kinetic resolution of epoxides **1–5** in the presence of  $\text{NaN}_3$ .<sup>a)</sup>

Epoxide	$ee_s$ (%)	$ee_p$ (%)	$E$
<b>1</b>	5	9	1
<b>2</b>	24	28	2
<b>3</b>	29	37	3
<b>4</b>	50	52	5
<b>5</b>	/	<1	1 <sup>[10c]</sup>

<sup>a)</sup> For experimental details see Tables S1 and S2.

Since the first HheB-catalysed transformations described in the literature were the ones with epichlorohydrin (**6**) and 1,3-dichloro-2-propanol (**7**) in the presence of sodium cyanide (Scheme 1),<sup>[6b]</sup> we decided first to test the wild-type HheB2 and five constructed mutants at those reactions (Table 2).

The difference in the optical purity of the formed (*R*)-4-chloro-3-hydroxybutyronitrile was observed, where HheB displayed the highest  $ee$  of 95%, while WT and variants Phe36Ile, Cys124Tyr and His125Gln were almost identical,  $ee = 76$ –78%. Variant Thr120Ala stems as superior to other single mutants, and comparable to HheB (Table 2A). When transformation starts from prochiral **7**, conversions and optical purities were enhanced to 99%  $ee$  with all enzymes, which could be attributed to two resolution steps, enantioselective dehalogenation of **7** followed by the ring-opening reaction of enantioenriched intermediate **6** (Table 2B). Overall, these results were encouraging giving some indication on the potential of B-group HHDHs to catalyse reactions in enantioselective fashion.

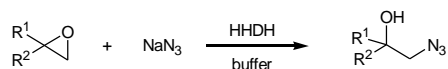
Next, a set of aliphatic epoxides was tested (Table 3). Reactions were carried out using sodium azide (Scheme 2). In general, in the ring-opening reaction azide ions give the highest activity compared to other nucleophiles (cyanide, cyanate, nitrite etc.). Enzymes were applied as a cell-free extract, being a suitable form for biocatalytic experiments. In the series of

**Table 2.** Formation of (*R*)-4-chloro-3-hydroxybutyronitrile from **6** (A) and **7** (B) catalysed by HheB2 variants.

HheB2 variant <sup>a</sup>	Conversion (%) <sup>c</sup>	<i>ee<sub>p</sub></i> (%) <sup>c</sup>	HheB2 variant <sup>b</sup>	Conversion (%) <sup>c</sup>	<i>ee<sub>p</sub></i> (%) <sup>c</sup>
Wild-type	18	76	Wild-type	80	99
Phe36Ile	20	78	Phe36Ile	90	99
His125Gln	20	76	His125Gln	91	99
Cys124Tyr	25	78	Cys124Tyr	77	99
Thr120Ala	24	90	Thr120Ala	75	99
HheB <sup>d</sup>	36	95	HheB <sup>d</sup>	91	99

<sup>a</sup>) Conditions A: substrate **6** (5 mM), NaCN (5 mM), 100  $\mu$ L cell-free extract, Tris-SO<sub>4</sub> buffer (20 mL, 50 mM, pH 7.5), 0.5% DMSO, total volume 21.2 mL, 4 h, 25  $^{\circ}$ C. For more details see Table S3. <sup>b</sup>) Conditions B: substrate **7** (5 mM), NaCN (15 mM), 100  $\mu$ L cell-free extract, Tris-SO<sub>4</sub> buffer (20 mL, 50 mM, pH 7.5), 0.4% DMSO, total volume 23.5 mL, 4 h, 25  $^{\circ}$ C. For more details see Tables S1 and S4. <sup>c</sup>) Determined by GC. <sup>d</sup>) quadruple mutant HheB2-Phe36Ile/Thr120Ala/Cys124Tyr/His125Gln identical to HheB.

aliphatic epoxides, the number and size of substituent were varied, covering substrates with one or two substituents at the chiral centre (terminal epoxides, **4** and **8–13**), as well as cyclohexene oxide (**14**) as a representative of 2,3-disubstituted oxiranes. From the eight epoxides tested, two remained intact (Table 3, entries 6 and 8). Two large substituents on the chiral centre (**12**) were not tolerated by HheB2 and its mutants, neither vicinal cyclic structure (**14**).

**Scheme 2.** Substrate screening on the azide-mediated ring-opening reaction.

This finding is in line with the previous observation that HheB2 does not catalyse the ring-opening of **14** with cyanide as a nucleophile.<sup>[9]</sup> Monosubstituted epoxides **4**, **8** and **9** were all converted with a high rate, high  $\beta$ -regioselectivity, and low to moderate (*S*)-enantioselectivity (Table 3, entries 1–3). As seen, HheB and mutant HheB2–Thr120Ala displayed a higher *E* value relative to wild-type and other mutants. In the case of those substrates, residues 36, 124 and 125 seem irrelevant for the enantioselectivity of the enzyme, while 120 appears the one contributing to the higher enantioselectivity of HheB, as also observed for **6** (Table 2).

**Table 3.** Enantioselectivity of HheB2 variants in the kinetic resolution of aliphatic epoxides.<sup>a</sup>

Entry	Epoxide	<i>E<sub>wild-type</sub></i>	<i>E<sub>Phe36Ile</sub></i>	<i>E<sub>His125Gln</sub></i>	<i>E<sub>Cys124Tyr</sub></i>	<i>E<sub>Thr120Ala</sub></i>	<i>E<sub>HheB</sub></i>	Config.
1	<b>4</b>	5	5	5	6	16	17	<i>S</i>
2	<b>8</b>	3	3	3	5	25	22	<i>S</i>
3	<b>9</b>	19	17	15	40	52	45	<i>S</i>
4	<b>10</b>	155	169	153	60	8	157	<i>R</i>
5	<b>11</b>	nd	nd	nd	nd	>200	>200	<i>R</i>
6	<b>12</b>	na	na	na	na	na	na	/
7	<b>13</b>	38	43	90	78	63	120	3 <i>R</i> ,5 <i>R</i>
8	<b>14</b>	na	na	na	na	na	na	/

<sup>a</sup>) Reactions were performed in Tris-SO<sub>4</sub> buffer (50 mM, pH 7.5) containing 0.5% DMSO, 5 mM (**4**, **8**, **9**, **10** and **13**) or 2 mM (**11**, **12** and **14**) substrate concentration, 5 mM NaN<sub>3</sub> and cell-free enzyme extract, total volume 21.3 mL, 25  $^{\circ}$ C. Reactions were monitored for up to 4 h. *E* values were calculated from *ee<sub>s</sub>* and *ee<sub>p</sub>*. nd = not determined due to very low activity. na = no activity observed. See Tables S1 and S6–S11 for more details.

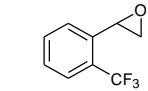
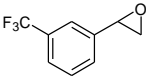
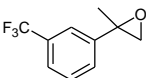
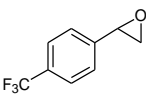
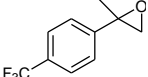
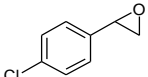
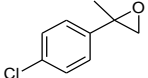
Introduction of methyl group on the chiral centre resulted in a huge increase of enantioselectivity for WT, Phe36Ile, His125Gln, HheB ( $E > 100$ ) and Cys124Tyr ( $E = 60$ ) for **10**, while the trend was inverted for the mutant Thr120Ala. Here, an unexpected and significant drop in enantioselectivity was found ( $E_{\text{Thr120Ala}} = 8$ ) relative to other enzymes (Table 3, entry 4). A positive influence of the methyl group as a second substituent was previously found with HheC,<sup>[14a]</sup> revealing the enzyme's potential to enable synthesis of tertiary alcohols. Interestingly, ethyl-homologue **11** was converted by both HheB and HheB2-Thr120Ala in a completely enantioselective fashion ( $E > 200$ ; Table 3, entry 5), while the wild-type and Phe36Ile, His125Gln and Cys124Tyr gave only traces of products.

In our previous studies, we described the activity of HDDHs on spiroepoxides.<sup>[15]</sup> Relative to HheA2, HheC showed much higher enantioselectivity towards spiroepoxide **13** ( $E = 3$  and  $E = 34$ , respectively). A comparable enantioselectivity to HheC<sup>[15]</sup> was found here in the reaction catalysed by HheB2 ( $E = 38$ ) as well as the same (*R*)-stereopreference, while all HheB2-mutants performed better than the wild-type (Table 3, entry 7). HheB showed not only higher enantioselectivity ( $E > 100$ ), but also higher activity (Table S11), and a great potential for the resolution of chiral spiroepoxides. On this series of substrates, HheB showed better biocatalytic properties compared to the HheB2, and could have wider application in the resolution of aliphatic epoxides.

A set of aromatic epoxides was evaluated next (Table 4). Styrene oxide derivatives with *ortho*-, *meta*- and *para*-substituents were included (**15**, **16**, **18**, **20**) as well as 2-methyl derivatives (**17**, **19**, **21**). Here, straightforward results were not obtained as with aliphatic epoxides. The common feature for all enzymes is that they are not active towards *o*-CF<sub>3</sub>-styrene oxide **15**. The lack of activity towards *ortho*-substituted styrene oxides was observed with several other HDDHs as well (unpublished results). Again, the second methyl group increases enantioselectivity relative to monosubstituted analogues (compare entries 2 and 3, 4 and 5, 6 and 7 in Table 4).

Among the four residues, position 36 seems irrelevant for the biocatalytic properties (Tables 3–4). Comparable results were obtained for all tested substrates with Phe36Ile and WT enzymes, which confirm that residue 36 on the protein surface does not influence enzyme's stereoselectivity. Among the three residues in the active site, positions 120 and 125 seem more important. Our results confirm the assumption of Watanabe et al. that Ala120 and Gln125 are responsible for the higher enantioselectivity of HheB compared to HheB2.<sup>[12]</sup> Their side chains are positioned close to the catalytic site, while the side chain of Tyr124 is located further (Figure 1). Yet, the impact of each mutation on the enantiodiscrimination seems to be substrate dependent. For monosubstituted aliphatic epoxides, similar performance of mutant HheB2-Thr120Ala and HheB is observed, while with aromatic substrates the His125Gln variant turns out to be comparable or in some cases even better than HheB.

**Table 4.** Enantioselectivity of HheB2 variants in the kinetic resolution of aromatic epoxides.<sup>a)</sup>

Entry	Epoxide	$E_{\text{wild-type}}$	$E_{\text{Phe36Ile}}$	$E_{\text{His125Gln}}$	$E_{\text{Cys124Tyr}}$	$E_{\text{Thr120Ala}}$	$E_{\text{HheB}}$	Config.
1	 <b>15</b>	na	na	na	na	na	na	/
2	 <b>16</b>	20	15	22	9	9	16	<i>S</i>
3	 <b>17</b>	nd	nd	114	nd	nd	111	<i>R</i>
4	 <b>18</b>	67	39	53	11	66	29	<i>R</i>
5	 <b>19</b>	>200	>200	>200	>200	>200	>200	<i>R</i>
6	 <b>20</b>	6	5	12	2	9	4	<i>R</i>
7	 <b>21</b>	>200	>200	>200	>200	>200	>200	<i>R</i>

<sup>a)</sup> Reactions were performed in Tris-SO<sub>4</sub> buffer (50 mM, pH 7.5) containing 5% DMSO, 2 mM substrate, 3 mM NaN<sub>3</sub> and 250 μL cell-free enzyme extract, total volume 2.5 mL, 25 °C. Reactions were monitored for up to 3 h.  $E$  values were calculated from  $ee_s$  and  $ee_p$ . nd = not determined due to very low activity. na = no activity observed. See Tables S1 and S12–S17 for more details.

Further experiments performed with benzyloxirane derivatives **22–24** showed the real catalytic potential and possible application of the B-group of HHDHs (Table 5). While 2-benzyloxirane **1** is converted to practically racemic product by WT, Phe36Ile, His125Gln and Cys124Tyr ( $E = 1–2$ ), and with slightly enhanced enantioselectivity by Thr120Ala and HheB ( $E = 12$ ) (Table 5, entry 1), introduction of a second substituent at the chiral centre led to a huge increase in enantioselectivity with  $E$  values above 100 (Table 5, entries 2–4), with one exception. Deterioration in enantioselectivity ( $E = 9$ ) was found in the reaction of **22** catalysed by HheB2-Thr120Ala (Table 5, entry 2), analogous behaviour observed previously with aliphatic substrate **10** (Table 3, entry 4). The effect of the Thr120Ala mutation will be discussed later.

Among the evaluated enzymes, HheB generally displayed superior performance. It is not only more enantioselective, but also active toward two more substrates (**11** and **17**) compared to HheB2. High activity towards benzyloxirane derivatives (**22–24**), substrates bearing aromatic substituent, is comparable to small aliphatic 1,2-epoxybutane (**4**) and 1,2-epoxyhexane (**8**) (Figure 2). Due to the high activity and enantioselectivity, HHDHs from B group showed to be a catalyst of choice for the resolution of those synthetically valuable molecules.

While HheC is an excellent catalyst for the resolution of 2-methyl-disubstituted epoxides,<sup>[15]</sup> replacement of the methyl group with a bulkier substituent like ethyl led to a significant drop in activity which can be explained by difficult placement of larger substrates into the relatively small active site of HheC (Figure S2). When tested under the same experimental conditions, no conversion of **11**, **23** and **24** was observed with HheC, while HheB2-enzymes tolerate such structural changes and catalyse reactions of **22–24** with both excellent activity and enantioselectivity (Table S22 and Figure S2). The explanation for the low enantioselectivity towards 1,2-epoxy-2-methylbutane observed earlier for HheB2,<sup>[9]</sup> can be found in slightly larger active site pocket compared to HheC.<sup>[12]</sup> Substrate that bears substituents with such a small difference in size have more freedom in HheB2, consequently the enzyme can accommodate

both enantiomers, which is not the case for HheC where fits only (*R*)-enantiomer.<sup>[9]</sup>

Interestingly, Zhang et al. have recently found the activity and enantioselectivity of HheC towards five-membered spiro-epoxyoxindoles and performed synthesis of a range of (*R*)-3-(azidomethyl)-3-hydroxyoxindoles with *ee* up to >99% at 30 mM substrate concentrations.<sup>[16]</sup> It is a nice example of how HHDHs can be efficiently applied on preparative scale resolution of spiroepoxide substrates and how enzymes from different organisms complement mutual catalytic repertoire.

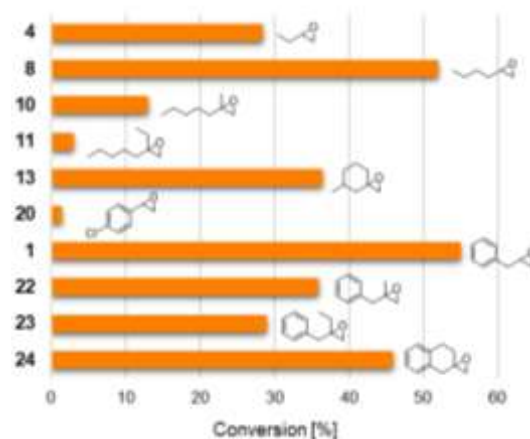


**Figure 2.** Conversion of selected epoxides in the azide-mediated ring-opening reaction catalysed by HheB. Reactions were performed in Tris-SO<sub>4</sub> buffer (50 mM, pH 7.5) containing DMSO (5% v/v), 2 mM substrate, 3 mM NaN<sub>3</sub> and HheB (10 μL), for 15 min at 25 °C, total volume 2.5 mL. For experimental details see Tables S1 and S21.

This study has revealed that the ability to convert 2,2-disubstituted epoxides in enantioselective fashion is not exclusive to HheC. HheB/HheB2-catalysed conversions of bulky 2,2-disubstituted epoxides, enable the biocatalytic synthesis of sterically challenging chiral tertiary alcohols in enantioselective fashion and show high potential for further process optimisation. The origins of high enantioselectivity towards 2,2-disubstituted epoxides **22–24**, were studied *in silico*.

**Table 5.** Enantioselectivity of HheB2 variants in the kinetic resolution of benzyloxirane derivatives.<sup>a)</sup>

Entry	Epoxide	$E_{\text{wild-type}}$	$E_{\text{Phe36Ile}}$	$E_{\text{His125Gln}}$	$E_{\text{Cys124Tyr}}$	$E_{\text{Thr120Ala}}$	$E_{\text{HheB}}$	Config.
1	<b>1</b>	1	1	1	2	12	12	<i>R</i>
2	<b>22</b>	>200	>200	>200	>200	9	>200	<i>R</i>
3	<b>23</b>	>200	>200	>200	>200	>200	>200	<i>R</i>
4	<b>24</b>	>200	196	172	>200	133	103	<i>R</i>

<sup>a)</sup> Reactions were performed in Tris-SO<sub>4</sub> buffer (50 mM, pH 7.5) containing 5% DMSO, 2 mM substrate, 3 mM NaN<sub>3</sub> and 10 μL cell-free enzyme extract, total volume 2.5 mL, 25 °C. Reactions were monitored for up to 2 h.  $E$  values were calculated from  $ee_s$  and  $ee_p$ . See Tables S1, S5 and S18–S20 for more details.

## Nucleophile scope

As in all HHDHs, the active site of HheB/HheB2 is made up of two main binding pockets; an epoxide-binding pocket and a halide-binding site which in HheC was shown to be capable of accepting a variety of non-natural nucleophiles including azide, cyanide, nitrite, cyanate, thiocyanate and formate ions.<sup>[2a]</sup> Similar to HheC, HheB has a spacious halide-binding site that can also accommodate anionic nucleophiles.<sup>[12]</sup> Activity with cyanide and azide ions was already confirmed within the group B,<sup>[6,10]</sup> while acceptance of other anions was not evaluated yet. We screened HheB2 with 7 nucleophiles (NaN<sub>3</sub>, NaNO<sub>2</sub>, NaCN, NaOCN, NaSCN, NaNO<sub>3</sub> and HCO<sub>2</sub>Na) in the ring-opening reaction by using benzyloxirane (**1**) as a model substrate, chosen due to high activity and chemical stability (Figure 3). As expected, azide gave the highest reaction rate, followed by nitrite (Figure 4). Comparable were activities with cyanide, cyanate and thiocyanate, although deceleration was observed during the course of cyanolysis, which is caused by product inhibition by cyanoalcohols (unpublished results). No products were observed when formate and nitrate ions were used. In addition, no product formation was detected in the absence of enzyme.

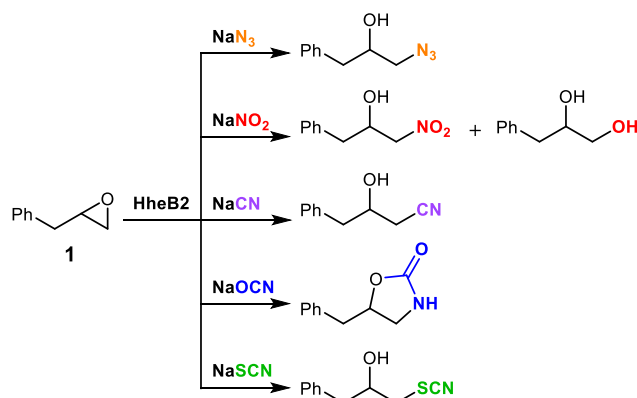


**Figure 3.** Nucleophile scope of HheB2-catalysed ring-opening reactions and products formed.

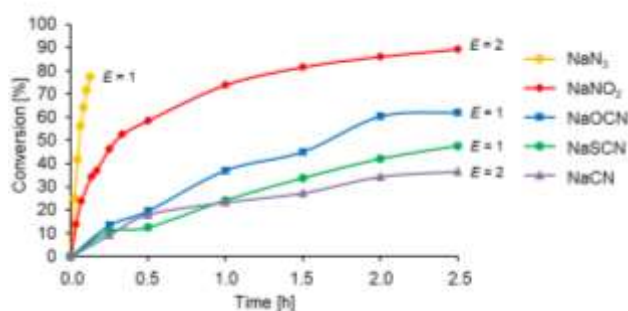


**Figure 4.** Progress curves of the ring-opening reaction of benzyloxirane (**1**) in the presence of different nucleophiles catalysed by HheB2 and calculated *E* values. For experimental details see Tables S1 and S23.

Although the conversion of **1** with all five nucleophiles proceeded with insignificant enantioselectivity (*E* = 1–2), still in each reaction a slight preference towards (*R*)-enantiomer was observed, indicating that stereopreference is not nucleophile-dependent. Ring-opening reactions proceeded with preferential attack of nucleophile at the less substituted carbon atom of oxirane ring ( $\beta$ -attack), in all cases with high regioselectivity. The formation of products was proven by GC-analysis using the synthesised reference material. As expected, reactions of **1** with NaN<sub>3</sub> and NaCN yielded 1-azido-3-phenylpropan-2-ol and 3-hydroxy-4-phenylbutanenitrile, respectively, while mixture of nitroalcohol and diol was obtained in the presence of NaNO<sub>2</sub>. Diol is formed by the attack of nitrite ion through oxygen atom followed by spontaneous hydrolysis.<sup>[2a]</sup> In the case of thiocyanate, the reaction took place via the sulphur atom yielding 1-phenyl-3-thiocyanatopropan-2-ol. Due to its instability, a small amount of corresponding thiirane was also detected in the reaction mixture. Particularly interesting is the reaction between the epoxide and cyanate ion that yields 2-oxazolidinone as the sole product. Intermediary isocyanate-cyanate species due to instability undergoes rapid cyclisation resulting in formation of synthetically valuable oxazolidinone. Previously, HheC and HheG were reported to catalyse synthesis of oxazolidinones, yet displaying opposite regioselectivity.<sup>[5b,14b]</sup> While HheC catalyses formation of 2-oxazolidinones, HheG catalyses formation of 4-oxazolidinones through the nucleophilic attack at the  $\alpha$ -position.

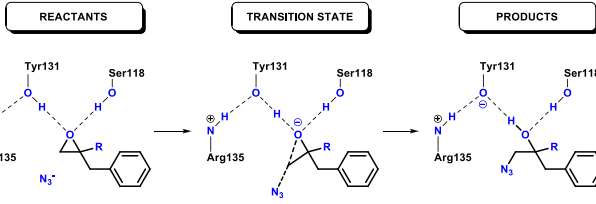
HheB displays similar nucleophile and activity profile, nevertheless a slightly higher enantioselectivity was noticed compared to HheB2 (Table S23). In addition, HheB2 exhibited substrate inhibition with all nucleophiles except azide ion. For those nucleophiles the maximum reaction velocities were between 10 and 20 mM (Figure S3), which should be considered during the process optimisation.

## Binding of substrates into the HheB active site

Computational analysis focused on the HheB enzyme and considered the most prominent substrates **22–24**, together with their unsubstituted analogue **1**, in revealing the origin of their enantioselectivity. To inspect a simple hypothesis that substrate affinities are determining trends in enzymatic reaction outcomes, we calculated the binding energy of epoxides and their 1-azido-2-alcohol products towards HheB with the established MM-GBSA analysis (Table 6), in line with our earlier reports.<sup>[17]</sup>

Obtained affinities suggest a favourable binding of all reactants, being an important prerequisite for a successful enzymatic conversion. Still, they do not point to any coherent trend that would, on its own, be able to interpret the determined *E* values.

**Table 6.** MM-GBSA binding affinities ( $\Delta G_{\text{BIND}}$ ) for epoxide reactants (R) and 1-azido-2-alcohol products (P), with activation ( $\Delta G^\ddagger$ ) and reaction free energies ( $\Delta G_{\text{R}}$ ) for their conversion based on the proposed mechanism within the HheB active site. All values are in kcal mol<sup>-1</sup>.



System	$\Delta G_{\text{BIND}}$		$\Delta G^\ddagger$	$\Delta G_{\text{R}}$
	R	P		
( <i>R</i> )- <b>1</b>	-11.4	-16.1	14.4	-28.1
( <i>S</i> )- <b>1</b>	-11.1	-13.2	14.4	-21.1
( <i>R</i> )- <b>22</b>	-11.5	-11.6	10.3	-34.5
( <i>S</i> )- <b>22</b>	-11.2	-12.0	19.1	-24.1
( <i>R</i> )- <b>23</b>	-11.3	-13.7	8.4	-20.9
( <i>S</i> )- <b>23</b>	-11.8	-12.0	21.9	-14.4
( <i>R</i> )- <b>24</b>	-12.3	-16.6	15.6	-22.0
( <i>S</i> )- <b>24</b>	-11.0	-17.2	19.6	-19.6

Specifically,  $\Delta G_{\text{BIND}}$  span a very narrow range, between -11.0 for (*S*)-**24** and -12.3 kcal mol<sup>-1</sup> for (*R*)-**24**, which is, on one hand, reasonable given a close structural similarity among substrates, but evidently unable to support a clear diversity in the *E* values. For example, values in Table 6 predict an identical difference of 0.3 kcal mol<sup>-1</sup> in favour of (*R*)-enantiomers for **1** and **22**, obviously disagreeing with a large difference in their *E* values, being 12 and exceeding 200, respectively. Still, one could argue that  $\Delta G_{\text{BIND}}$  indicate a stronger binding for (*R*)-enantiomers in **1**, **22** and **24**, which could sustain a potential assumption that larger affinities lead to a better conversion. Yet, the opposite is observed for **23**, which, knowing it reveals one of the best enantiomeric profiles, eliminates this aspect as dominant in governing the overall enzyme enantioselectivity. Therefore, we can derive a firm conclusion that, although  $\Delta G_{\text{BIND}}$  appear accurate in relative terms, the affinity of HheB towards its substrates/products is not predominantly determining the reaction outcomes, which, instead, likely resides in the kinetic and thermodynamic parameters of reactions within the enzyme.

We feel the latter conclusion is especially true knowing that identified binding poses seem correct and are found within what is expected for these enzymes (Figure 5). Specifically, all (*R*)-enantiomers are positioned in the active site in a way that allows the hydrogen bonding formation among their epoxide O-atoms and the side chains of the catalytic residues Tyr131 and Ser118, as demonstrated in the literature.<sup>[14a,18]</sup> This aspect can help in rationalizing the preference of HheB in affording (*R*)-products as predominant in all substrates. In contrast, for (*S*)-analogues, the productive orientation is observed only for **1**, while the most favourable position for **22–24** reveals that other residues are more important for their

binding (Figure 5B), which likely leads to their slower conversion.

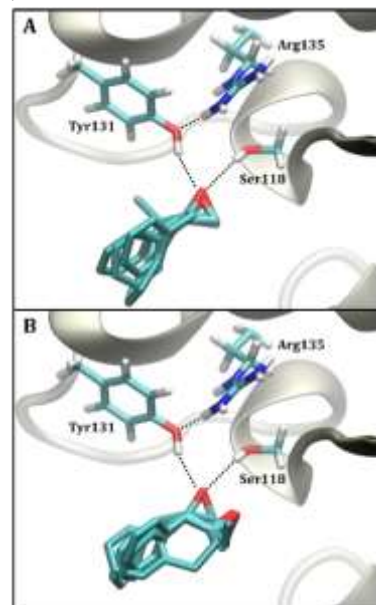


**Figure 5.** Overlap of the identified binding positions for (*R*)-substrates (in A) and (*S*)-substrates (in B) indicating a productive orientation of all (*R*)-substrates and (*S*)-**1**.

Lastly, we note in passing that MM-GBSA analysis consistently predicts higher product affinities over those for initial reactants, which even appears reasonable given that a rigid cyclic epoxide is converted to a flexible open-form alcohol, additionally possessing the introduced azide moiety, which jointly optimize interactions with the active site residues. Still, at first, this notion might point to the inability of substrates to displace products from the active site, leading to the enzyme inhibition. This ambiguity is resolved knowing that the calculated enzyme reaction free energies are much more exergonic than product affinities (Table 6). The latter, then, compensate high energy requirements to liberate products into solution, and allow only a modest product inhibition (unpublished results), thereby firmly confirming experimental results.

The presented analysis strongly points to the absence of any consistent relation between the ability of reacting epoxides or produced 1-azido-2-alcohols to bind HheB and the efficiency of their enantioselective resolution, which precisely matches conclusions from similar earlier reports.<sup>[18]</sup> Still, if the most favourable docking binding poses, for both reactants and products, are submitted to MD simulations, the attained trajectories reveal a tendency of all systems to depart the enzyme, rather than to remain within its binding pocket (Figure S6). Without going into detail, this interesting insight seems to suggest that, despite reaching superb enantioselectivity with several derivatives, the most profound substrates, **22–24**, can hardly be described as optimal for the considered HheB enzyme. Therefore, this promising framework for the enantioselective resolution is likely to identify even better substrates in our ongoing future research.

## Enzymatic reaction in the HheB active site

Preceding analysis clearly showed that different enantioselectivities are originating in altered thermodynamic and kinetic parameters of reactions in the HheB active site. To evaluate that, we modelled the precise reaction mechanism for the conversion of considered epoxides into 1-azido-2-alcohols (Table 6).

The investigated process relies on a simple mechanism with the following steps: (1) An epoxide is anchored in the active site by two O–H···O hydrogen bonds involving its epoxide oxygen and the side chain –OH groups from Tyr131 and Ser118; (2) A nucleophilic azide approaches the epoxide towards its C( $\beta$ )-atom, which elongates the C( $\beta$ )–O bond and leads to the transition state structure (Figure S7) with typical N(azide)–C( $\beta$ ) and C( $\beta$ )–O bonds of 2.0 and 1.7 Å, respectively; (3) Following the transition state formation, the reaction offers 1-azido-2-alkoxides, which get reverted to neutral alcohols by a proton transfer from Tyr131. The latter prevails over Ser118 in this respect, given a typically higher acidity of phenols over alcohols.<sup>[19]</sup> The mentioned proton transfer is further assisted by Arg135, which stabilizes the formed Tyr131 phenoxide through the N–H···O hydrogen bond.

In all cases, the inspected processes are highly exergonic, with the reaction Gibbs free energies between  $-14.4$  kcal mol<sup>-1</sup> for (*S*)-**23** and  $-34.5$  kcal mol<sup>-1</sup> for (*R*)-**22**. This suggests a high feasibility of all reactions, and confirms the validity of the considered mechanism. Also,  $\Delta G_R$  values are consistently more favourable for (*R*)-enantiomers, which already hints at their dominance among products. Interestingly, the calculated kinetic barriers for **1** are precisely identical among enantiomers, both at  $\Delta G^\ddagger = 14.4$  kcal mol<sup>-1</sup>, found in line with a revealed productive orientation of both enantiomers in this case (Figure 5), being the lowest activation energy among (*S*)-substrates, and, at the same time, the second highest for all considered (*R*)-analogues. This suggests an equal HheB efficiency to convert both enantiomers, yet a slight dominance in the formed (*R*)-product can be expected from its somewhat higher reaction exergonicity of  $-7.0$  kcal mol<sup>-1</sup>. This is in agreement with experiments, as equal kinetic aspects joined with minor reaction free energy differences, suggest only a moderate *E* value, thus confirming the measured value of only 12 for **1**. Kinetic differences among enantiomers start to appear in **24**, where its (*R*)-analogue exhibits 4.0 kcal mol<sup>-1</sup> lower barrier and 2.4 kcal mol<sup>-1</sup> higher reaction exergonicity. This hints at a higher *E*, thus tying our results with the increased value of around 100. An even larger difference in the activation free energies are obtained for **22** (8.8 kcal mol<sup>-1</sup>) and especially **23** (13.5 kcal mol<sup>-1</sup>) that parallel their thermodynamic preference,  $-10.4$  kcal mol<sup>-1</sup> for **22** and  $-6.5$  kcal mol<sup>-1</sup> for **23**, which both predict an almost exclusive formation of the matching (*R*)-products. This supports experimentally determined *E* values exceeding 200,

therefore revealing an excellent agreement among both sets of data.

As an attractive observation, we note a correlation between the obtained *E* values and the height of the kinetic barrier for (*R*)-enantiomers. Namely, the *E* values for selective and prominent **22–24** increase in the order **24** < **22**  $\approx$  **23**, which is followed by a decrease in the calculated  $\Delta G^\ddagger$  values, being 15.6, 10.3 and 8.4 kcal mol<sup>-1</sup>. This indicates that a faster reaction leads to a better enantioselectivity, which confirms a kinetic resolution. Still, to elucidate HheB structural determinants leading to a barrier reduction, we have utilized the decomposition analysis of  $\Delta G_{\text{BIND}}$  values (Table S27). We noticed that catalytic residues, Tyr131, Ser118 and Arg135, dominate the binding of all enantiomers, except (*R*)-**1** and (*S*)-**22**, which could lead to a minor enantioselectivity in **1**, and a very pronounced one in **22**. Other than those, we identified Tyr169 as important for the observed HheB activities (Figure 6). Namely, data in Table S27 suggest that the activation barrier reduction also follows individual contributions from Tyr169 in the binding of (*R*)-enantiomers. In other words, for less enantioselective **1** and **24**, these are  $-1.39$  and  $-1.53$  kcal mol<sup>-1</sup>, respectively, and increase to  $-1.78$  and  $-2.05$  kcal mol<sup>-1</sup> for **22** and **23**, thus making Tyr169 the most dominant residue for the binding. These correspond to C–H··· $\pi$  interactions that the –CH<sub>2</sub>– group from the epoxide C( $\beta$ )-atom makes with the Tyr169 phenyl side chain, where we notice that larger and bulkier alkyl substituents facilitate these contacts. This holds especially for flexible moieties, –Me in **22** and –Et in **23**, and somewhat less for more rigid cyclic system **24**. Hence, based on these results, we propose Tyr169 as an important residue for the outcome of the HheB catalysis.

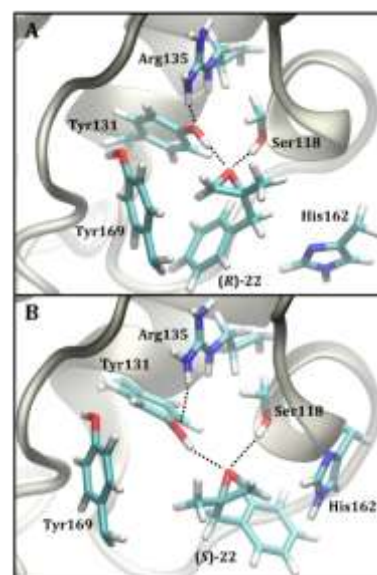


**Figure 6.** An enlarged view of the active site for (*R*)-**22** (in A) and (*S*)-**22** (in B) showing the importance of Tyr169 for the binding of (*R*)-**22** and His162 for (*S*)-**22**.

**Table 7.** MM-GBSA binding affinities ( $\Delta G_{\text{BIND}}$ ) and their decomposition (in kcal mol<sup>-1</sup>) for four residues mutated in HheB2 and its variant with only the Thr120Ala mutation.

System	$\Delta G_{\text{BIND}}$	HheB2 with 4 mutations (HheB)				
		Ile36	Ala120	Thy124	Gln125	SUM
( <i>R</i> )- <b>22</b>	-11.5	0.0	-0.6	-0.1	-0.6	-1.3
( <i>S</i> )- <b>22</b>	-11.2	0.0	-0.2	0.0	-0.3	-0.5
System	$\Delta G_{\text{BIND}}$	HheB2 with a Thr120Ala mutation				
		Phe36	Ala120	Cys124	His125	SUM
( <i>R</i> )- <b>22</b>	-11.2	0.0	-0.4	-0.1	-0.3	-0.8
( <i>S</i> )- <b>22</b>	-11.7	0.0	-0.2	-0.1	-0.1	-0.4

Computational analysis also justified the strategy to utilize epoxides through revealing their insensitivity towards azides outside the enzyme active site, while their preceding 1-halo-2-alcohols readily give 1-azido derivatives in the aqueous solution in a racemic fashion (see discussion in Supporting Information), which is not desirable.

Lastly, we focused on offering some insight into a significant drop in the enantioselectivity for **22**, from  $E > 200$  to  $E = 9$ , once HheB is replaced with its analogue having only the Thr120Ala mutation (Tables 3 and 5). Since the crystal structure of the employed native HheB2 enzyme from *Mycobacterium* sp. is not available, we relied on the utilized HheB structure, where we have manually reverted Ile36, Tyr124 and Gln125 into their native counterparts, Phe36, Cys124 and His125, while maintaining the Thr120Ala mutation. Following the docking and MD simulations of both enantiomers of **22**, we compared the decomposition of MM-GBSA binding energies, particularly concentrating on the crucial four residues that make a difference among variants (Table 7). It appears that the enantioselectivity reduction is prompted by two contributions. Namely, the HheB2-Thr120Ala variant changes the trend in  $\Delta G_{\text{BIND}}$  among enantiomers, being by  $-0.3$  kcal mol<sup>-1</sup> higher for the (*R*)-analogue in HheB, while is reverted to a  $-0.5$  kcal mol<sup>-1</sup> higher affinity for the (*S*)-enantiomer in the Thr120Ala variant. Still, the crucial role lies in the increased kinetic requirement for the conversion of (*R*)-**22**, from  $\Delta G^\ddagger = 10.3$  kcal mol<sup>-1</sup> in HheB to  $\Delta G^\ddagger = 16.2$  kcal mol<sup>-1</sup> in Thr120Ala, while leaving it practically intact for (*S*)-**22**, thus reducing the kinetic difference among enantiomers. The latter leads to a large enantioselectivity decline and confirms the importance of kinetic aspects for the enantiomeric distribution of products.

## Conclusion

To further improve and extend the scope of HDDH-catalysed reactions, a more efficient and more enantioselective enzymes are required. One option is to modify natural enzymes through engineering/directed evolution. The alternative is extensive substrate screening of already discovered HDDHs from wild-type sources, as represented in this work. Although, the enzyme HheB2 from

*Mycobacterium* sp. has been previously characterised as a non-enantioselective enzyme, this study has revealed its biocatalytic value. Despite relatively poor performance on the majority of substrates, enzymes from the group B work excellently on sterically demanding 2,2-disubstituted epoxides. This makes them valuable new catalysts in the portfolio of enantioselective enzymes for synthesis of optically pure bulky tertiary alcohols, important chiral synthons. Due to observed substrate inhibition, a proper process optimization should be carried out in the future to achieve the full biotechnological potential of these enzymes.

Computational analysis demonstrated a complete lack of any correlation between binding affinities of either reacting epoxides or formed products with the observed enantioselectivities, thereby ruling out these aspects as dominant. In contrast, the calculated kinetic and thermodynamic parameters of reactions occurring within the enzyme active site nicely explained an increased enantioselectivity in substrates **22–24**, relative to their unsubstituted analogue **1**, and demonstrated the significance of Tyr169 along with the catalytic residues Tyr131, Ser118 and Arg135 for the reaction outcomes.

A site-directed mutagenesis and molecular modelling studies allowed identifying residues important for chiral recognition, which is a good starting point for further protein engineering studies directed toward further broadening of the substrate spectrum.

## Experimental Section

### General information

<sup>1</sup>H and <sup>13</sup>C NMR spectra were recorded on a Bruker AV 300 and 600 (<sup>1</sup>H 300 or 600 MHz and <sup>13</sup>C 75 or 151 MHz) spectrometers in CDCl<sub>3</sub>. Chemical shifts ( $\delta$ ) are given in ppm downfield from TMS as the internal standard. Coupling constants are given in Hz. High resolution mass spectrometry (HRMS) was performed on 4800 Plus MALDI TOF/TOF Analyzer (CHCA matrix). Enzymatic reactions were monitored by gas chromatography (GC) using an Agilent instrument 8860 GC Systems equipped with a FID detector (set at 300 °C) and a split injector (set at 250 °C) and N<sub>2</sub> as the carrier gas and an autosampler. Analyses were performed using commercially available columns HP-5 (30 m x 0.25 mm x 0.25  $\mu$ m, Agilent) or HP-1 (60 m x 0.25 mm x 0.25  $\mu$ m, Agilent), Table S24. The optical purity of the

formed products was determined by chiral GC or HPLC analysis (Tables S25 and S26). HPLC analysis was performed on an Agilent 1260 Infinity instrument. Column chromatography was done using silica gel (Merck type 9385, 230-400 mesh). TLC was performed on 0.25 mm silica gel 60-F plates (Merck). The commercial grade reagents and solvents were used without further purification. Racemic substrates (2,3-epoxypropyl)benzene (**1**), styrene oxide (**2**), allyl glycidyl ether (**3**), 1,2-epoxybutane (**4**), epichlorohydrin (**6**), 1,3-dichloro-2-propanol (**7**), 1,2-epoxyhexane (**8**) and cyclohexene oxide (**14**), as well as trimethylsulfoxonium iodide, trimethylsulfonium iodide, KO<sup>t</sup>Bu, NaH (60% dispersion in mineral oil), azidotrimethylsilane, (*R,R*)-*N,N*-bis(3,5-di-*tert*-butylsalicylidene)-1,2-cyclohexanediaminochromium(III) chloride were supplied by Aldrich. 3,3-Dimethyl-1,2-epoxybutane (**9**), 4-chlorostyrene oxide (**20**), 2-methyl-3-phenyl propene, 2-tetralone, NaN<sub>3</sub> and NH<sub>4</sub>Cl were purchased from Alfa Aesar. 2'-trifluoromethylacetophenone, 3'-trifluoro-methylacetophenone, 4'-trifluoromethylacetophenone, 2-trifluoromethylbenzaldehyde, 3-trifluoromethylbenzaldehyde, 4'-chloroacetophenone were purchased from AK Scientific. L-Arabinose, ampicillin sodium salt, β-mercaptoethanol, glycerol and EDTA were purchased from Carl Roth. Bacto-tryptone, yeast extract and bacto-agar were purchased from Difco. Complete Protease Inhibitor Cocktail Tablets were supplied by Roche. Sorbitol was from Sigma, while NaCN was obtained from Kemika. Water was purified with a Millipore (Bedford, MA) Milli-Q water system. (3*R*,5*R*),(3*S*,5*S*)-5-Methyl-1-oxaspiro[2.5]octane **13**<sup>[15]</sup> and *rac*-2-(4-(trifluoromethyl)phenyl)oxirane **18**<sup>[20]</sup> were prepared as previously described.

### Site-directed mutagenesis

Using the pBAD HheB2 as template, four single mutants were obtained by PCR site-directed mutagenesis method with synthesized primers to replaced codons as Thr120Ala, Phe36Ile, Cys124Tyr, His125Gln. Then the Phe36Ile were used as templates for PCR reaction to construct double mutant (Phe36Ile/Thr120Ala), and double mutant were used as templates to construct quadruple mutant identical to HheB (simultaneous mutations at adjacent sites 124 and 125).

Each 25 μl PCR contained 25 ng of the DNA template, 0.2 mM dNTPs each, 0.4 μM of the forward and reverse primers and 0.25U Q5 polymerase in the Q5 reaction buffer (Thermo). The following cycling protocol was used: initial denaturation for 30 s at 98 °C; 30 cycles of denaturation for 15 s at 98 °C, annealing for 30 s at 60 °C and polymerization for 3 min at 72 °C; Final extension for 2 min at 72 °C. The results of the PCR reaction were assessed by agarose gel electrophoresis. If the reaction was successfully done, the product of the PCR reaction was subjected to Dpn I treatment to dispose of the maternal template. The 10 μl PCR products were incubated with 0.2 μl of DpnI enzyme in Cutsmart buffer (New England Biolabs) for overnight at 37 °C. The following pairs of primers were used in this study, the mutated codons are underlined:

Phe36Ile-For5'-CAGAGGTCATCGCTGACCACAC-3',  
 Phe36Ile-Rev5'-GTGTGGTCAGCGATGACCTCTG-3',  
 Thr120Ala-For5'-CTACGGAAGTGCCGCAGCGATG-3',  
 Thr120Ala-Rev5'-CATCGTCGGGCACTTCCGTAG-3',  
 Cys124Tyr-For5'-CGATGCGGTTACCATGAAGGTGC-3',  
 Cys124Tyr-Rev5'-GCACCTTCATGGTACCGCATCG-3',  
 His125Gln-For5'-GATGCGGTACCAAAGAAGGTG-3',  
 His125Gln-Rev5'-CACCTTCTGGTACCGCATC-3',  
 Cys124Tyr/His125Gln-For5'-  
 CGATGCGGTACCAAGAAGGTGC-3',  
 Cys124Tyr/His125Gln-Rev5'-  
 GCACCTTCTGGTACCGCATCG-3'.

### Enzyme expression

Enzymes were prepared by overexpression in *E. coli* strain MC1061 according to a previously described protocol<sup>[10c]</sup> and used as cell-free extract. The concentration of protein determined by using Bradford's method was 2.8 mg/ml for HheB2 and 2.3-3.0 mg/ml for mutants (Table S1). The protein profile of the obtained extract was analysed by SDS-PAGE (Figure S1).

### Kinetic resolution experiments – general procedure

To Tris-SO<sub>4</sub> buffer (50 mM, pH 7.5) a stock solution of epoxide in DMSO was added at 25 °C (final concentration 2-5 mM for aliphatic and 2 mM for aromatic epoxides), followed by addition of a stock solution of NaN<sub>3</sub> in water (final concentration 3 mM or 5 mM). Reactions were initiated by addition of cell-free extract (protein concentrations between 2.3 and 3.0 mg/ml) in the TEMG buffer. The progress of the reaction was followed by periodically taking samples (0.5 mL) from the reaction mixture. Samples were extracted with MTBE (1.0 mL) containing mesitylene as internal standard and analysed by GC for conversion and product identification. In parallel, chiral GC and/or HPLC analyses were performed to determine the enantiomeric purity of the product and remaining substrate. The spontaneous reactions of epoxides **1–24** with NaN<sub>3</sub> were followed by monitoring epoxide consumption in the absence of enzyme.

### Nucleophile screening

To Tris-SO<sub>4</sub> buffer (50 mM, pH 7.5) a stock solution of **1** in DMSO was added to final concentration of 2 mM, followed by addition of a stock solution of NaN<sub>3</sub>, NaCN, NaNO<sub>2</sub>, NaOCN, NaSCN, NaNO<sub>3</sub> or HCO<sub>2</sub>Na in water (final conc. 3 mM). Reactions were initiated by addition of cell-free extract in the TEMG buffer (200-400 μL HheB2 or HheB). The progress of the reaction was followed by periodically taking samples (0.5 mL) from the reaction mixture. Samples were extracted with MTBE (1.0 mL) containing mesitylene as internal standard and analysed by GC for conversion and product identification. In parallel, chiral GC and/or HPLC analyses were performed to determine the enantiomeric purity of the product and remaining substrate. The spontaneous reactions of epoxide **1** with NaNu were followed by monitoring epoxide consumption and product formation in the absence of enzyme.

### Acknowledgements

This work was financially supported by CAT PHARMA (KK.01.1.1.04.0013), a project co-financed by the Croatian Government and the European Union through the European Regional Development Fund - the Competitiveness and Cohesion Operational Programme. We would like to acknowledge the use of the equipment provided by CroBioPro (KK.01.1.1.01.0002). L.H. wishes to thank the Croatian Science Foundation for a doctoral stipend through the Career Development Project for Young Researchers.

### References

- [1] a) Z. Findrik Blažević, N. Milčić, M. Sudar, M. Majerić Elenkov, *Adv. Synth. Catal.* **2021**, *363*, 388–410; b) A. Schallmeyer, M. Schallmeyer, *Appl. Microbiol. Biotechnol.* **2016**, *100*, 7827–7839.
- [2] a) G. Hasnaoui-Dijoux, M. Majerić Elenkov, J. H. Lutje Spelberg, B. Hauer, D. B. Janssen, *ChemBioChem* **2008**, *9*, 1048–1051; b) M. Majerić

- Elenkov, W. Szymański, D. B. Janssen, in *Science of Synthesis, Biocatalysis in Organic Synthesis 2, Vol. 2* (Eds.: K. Faber, W.-D. Fessner, N. J. Turner), Thieme, Stuttgart, **2014**, pp. 507–527.
- [3] J. Koopmeiners, B. Halmschlag, M. Schallmeyer, A. Schallmeyer, *Appl. Microbiol. Biotechnol.* **2016**, *100*, 7517–7527.
- [4] a) J. H. Lutje Spelberg, J. E. van Hylckama Vlieg, L. Tang, D. B. Janssen, R. M. Kellogg, *Org. Lett.* **2001**, *3*, 41–43; b) W. Szymanski, C. P. Postema, C. Tarabiono, F. Berthiol, L. Campbell-Verduyn, S. de Wildeman, J. G. de Vries, B. L. Feringa, D. B. Janssen, *Adv. Synth. Catal.* **2010**, *352*, 2111–2115; c) R. M. Haak, C. Tarabiono, D. B. Janssen, A. J. Minnaard, J. G. de Vries, B. L. Feringa, *Org. Biomol. Chem.* **2007**, *5*, 318–323; d) N. Wan, X. Zhou, R. Ma, J. Tian, H. Wang, B. Cui, W. Han, Y. Chen, *Adv. Synth. Catal.* **2020**, *362*, 1201–1207.
- [5] a) E. Calderini, J. Wessel, P. Süß, P. Schrepfer, R. Wardenga, A. Schallmeyer, *ChemCatChem* **2019**, *11*, 2099–2106; b) N. Wan, J. Tian, X. Zhou, H. Wang, B. Cui, W. Han, Y. Chen, *Adv. Synth. Catal.* **2019**, *361*, 4651–4655; c) F. Xue, X. Ya, Q. Tong, Y. Xiu, H. Huang, *Process Biochem.* **2018**, *75*, 139–145; d) F. Xue, Z.-Q., Liu, Y.-J. Wang, N.-W. Wan, Y.-G. Zheng, *J. Mol. Catal. B: Enzym.* **2015**, *115*, 105–112; e) L. Martinez-Montero, D. Tischler, P. Süß, A. Schallmeyer, M. C. R. Franssen, F. Hollmann, C. F. Paul, *Catal. Sci. Technol.* **2021**, *11*, 5077–5085; f) X.-Y. Zhou, N.-W. Wan, Y.-N. Li, R. Ma, B.-D. Cui, W.-Y. Han, Y.-Z. Chen, *Adv. Synth. Catal.* **2021**, *363*, 4343–4348; g) J.-F. Wu, N.-W. Wan, Y.-N. Li, Q.-P. Wang, B.-D. Cui, W.-Y. Han, Y.-Z. Chen, *iScience* **2021**, *24*, 102883.
- [6] a) T. Nakamura, T. Nagasawa, F. Yu, I. Watanabe, H. Yamada, *Tetrahedron* **1994**, *50*, 11821–11826; b) T. Nakamura, T. Nagasawa, Y. Fujio, I. Watanabe, H. Yamada, *Biochem. Biophys. Res. Comm.* **1991**, *180*, 124–130.
- [7] a) G. J. Poelarends, J. E. T. van Hylckama Vlieg, J. R. Marchesi, L. M. F. Dos Santos, D. B. Janssen, *J. Bacteriol.* **1999**, *181*, 2050–2058; b) J. E. T. van Hylckama Vlieg, L. Tang, J. H. Lutje Spelberg, T. Smilda, G. J. Poelarends, T. Bosma, A. E. J. van Merode, M. W. Fraaije, D. B. Janssen, *J. Bacteriol.* **2001**, *183*, 5058–5066.
- [8] J. H. Lutje Spelberg, L. Tang, M. van Gelder, R. M. Kellogg, D. B. Janssen, *Tetrahedron: Asymmetry*, **2002**, *13*, 1083–1089.
- [9] M. Majerić Elenkov, B. Hauer, D. B. Janssen, *Adv. Synth. Catal.* **2006**, *348*, 579–585.
- [10] a) B. Seisser, I. Lavandera, K. Faber, J. H. Lutje Spelberg, W. Kroutil, *Adv. Synth. Catal.* **2007**, *349*, 1399–1404; b) J. H. Schrittwieser, I. Lavandera, B. Seisser, B. Mautner, W. Kroutil, *Eur. J. Org. Chem.* **2009**, *2009*, 2293–2298; c) M. Majerić Elenkov, M. Čičak, A. Smolko, A. Knežević, *Tetrahedron Lett.* **2018**, *59*, 406–408.
- [11] F. Watanabe, F. Yu, A. Ohtaki, Y. Yamanaka, K. Noguchi, M. Odaka, M. Yohda, *J. Biosci. Bioeng.* **2016**, *122*, 270–275.
- [12] F. Watanabe, F. Yu, A. Ohtaki, Y. Yamanaka, K. Noguchi, M. Yohda, M. Odaka, *Proteins* **2015**, *83*, 2230–2239.
- [13] M. Estévez-Gay, J. Iglesias-Fernández, S. Osuna, *Catalysts* **2020**, *10*, 1403.
- [14] a) M. Majerić Elenkov, L. Tang, B. Hauer, D. B. Janssen, *Adv. Synth. Catal.* **2007**, *349*, 2279–2285; b) M. Majerić Elenkov, L. Tang, A. Meetsma, B. Hauer, D. B. Janssen, *Org. Lett.* **2008**, *10*, 2417–2420; c) C. Molinaro, A. A. Guilbault, B. Kosjek, *Org. Lett.* **2010**, *12*, 3772–3775.
- [15] M. Majerić Elenkov, I. Primožič, T. Hrenar, A. Smolko, I. Dokli, B. Salopek-Sondi, L. Tang, *Org. Biomol. Chem.* **2012**, *10*, 5063–5072.
- [16] F.-R. Zhang, N.-W. Wan, J.-M. Ma, B.-D. Cui, W.-Y. Han, Y.-Z. Chen, *ACS Catal.* **2021**, *11*, 9066–9072.
- [17] a) L. Hok, H. Rimac, J. Mavri, R. Vianello, *Comput. Struct. Biotechnol. J.* **2022**, *20*, 1254–1263; b) L. Hok, J. Mavri, R. Vianello, *Molecules* **2020**, *25*, 6017; c) M. Marinović, G. Poje, I. Perković, D. Fontinha, M. Prudêncio, J. Held, L. Pessanha de Carvalho, T. Tandarić, R. Vianello, Z. Rajić, *Eur. J. Med. Chem.* **2021**, *224*, 113687.
- [18] R. M. de Jong, J. J. W. Tiesinga, A. Villa, L. Tang, D. B. Janssen, B. W. Dijkstra, *J. Am. Chem. Soc.* **2005**, *127*, 13338–13343.
- [19] S. Tshepelevitsh, A. Kütt, M. Lökov, I. Kaljurand, J. Saame, A. Heering, P. Plieger, R. Vianello, I. Leito, *Eur. J. Org. Chem.* **2019**, *40*, 6735–6748.
- [20] I. Dokli, N. Milčić, P. Marin, M. Svetec Miklenić, M. Sudar, L. Tang, Z. Findrik Blažević, M. Majerić Elenkov, *Catal. Commun.* **2021**, *152*, 106285.

## RESEARCH ARTICLE

## Expanding the Scope of Enantioselective Halohydrin Dehalogenases – Group B

*Adv. Synth. Catal.* **Year**, *Volume*, Page – Page

Emina Mehić, Lucija Hok, Qian Wang, Irena Dokli, Marina Svetec Miklenić, Zvezdana Findrik Blažević, Lixia Tang, Robert Vianello,\* Maja Majerić Elenkov\*

